

Supporting Information

Planting Carbon Nanotubes onto Supramolecular Polymer Matrixes for Waterproof Non-Contact Self-Healing

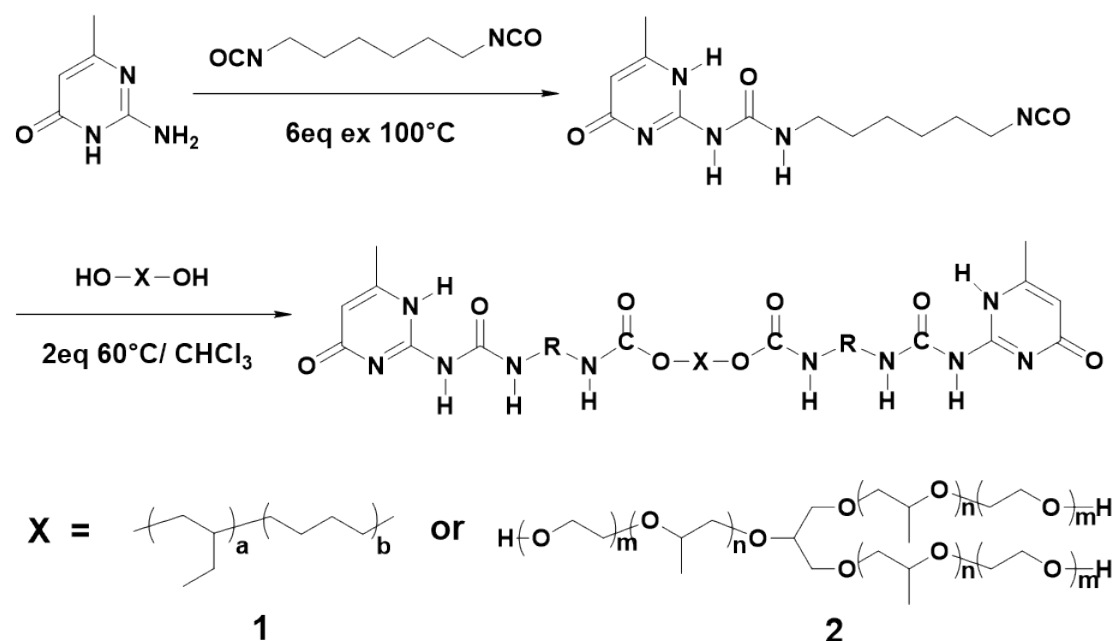
Bo Li,^a Lei Kan,^a Shuai Zhang,^a Zhengdao Liu,^a Chao Li,^b Wei Li,^b Xinyue Zhang,^{a,*} Hao Wei^a and Ning Ma^{a,*}

^a Key Laboratory of Superlight Material and Surface Technology of Ministry of Education, College of Material Science and Chemical Engineering, Harbin Engineering University, Harbin, 150001, China.

^b College of Automation, Harbin Engineering University, Harbin, 150001, China.

E-mail: xinyue@hrbeu.edu.cn (X.Z.); nma@hrbeu.edu.cn (N.M.)

1. Experimental details of supramolecular polymers



Scheme S1 Synthetic route of supramolecular polymers.

2(6-isocyanatohexylaminocarbonylamino)-6-methyl-4[1H]-pyrimidinone

¹H NMR (ppm, 500 MHz, CDCl₃): δ 13.1 (s, 1H), 11.9 (s, 1H), 10.2 (s, 1H), 5.8 (s, 1H), 3.3 (m, 4H), 2.2 (s, 3H), 1.6 (m, 4H), 1.4 (m, 4H).

FT-IR (neat): ν (cm⁻¹) 1255, 1524, 1578, 1667, 1699, 2283, 3233, 3466.

N,N'-Bis-{6-(4[1H]-oxo-pyrimidinyl-6-methyl-2-ureido)hexylureido}-poly(ethylene-butylene) (1)

¹H NMR (ppm, 500 MHz, CDCl₃): δ 13.1, 11.9, 10.2, 5.8, 4.1, 3.3-3.0, 2.9-2.8, 2.2, 1.6-1.0, 0.8.

FT-IR (neat): ν (cm⁻¹) 3457, 3336, 3216, 2959, 2925, 2855, 1700, 1664, 1590, 1525, 1461, 1379, 1252, 761.

N,N'-Bis-{6-(4[1H]-oxo-pyrimidinyl-6-methyl-2-ureido)hexylureido}-tripoly(propylene glycol)-block-poly(ethylene glycol) (2)

¹H NMR (ppm, 500 MHz, CDCl₃): δ 13.1, 11.8, 10.2, 8.0, 4.2, 3.8-3.1, 2.3, 1.7-1.0.

FT-IR (neat): ν (cm⁻¹) 3341, 3216, 2971, 2931, 2869, 1722, 1700, 1667, 1588, 1527, 1454, 1374, 1256, 1108, 1015, 931.

2. Basic characterizations of SP1, SP2 supramolecular polymers and their blended films

The FT-IR spectra (Fig. S1) showed that the 85:15 blended samples had the characteristic absorption peaks of SP1 and SP2.

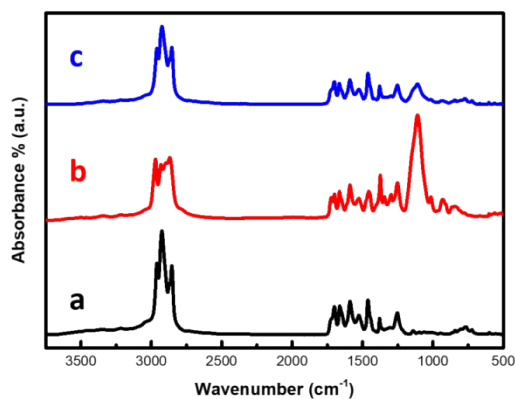


Fig. S1 The FT-IR spectra of (a) SP1, (b) SP2, (c) 85:15 SP1: SP2 samples.

Rheology test curves of SP1, SP2 and 85:15 SP1:SP2 sample were shown in Fig.S2. The dynamic oscillatory frequency sweep of the SP1, SP2 and 85:15 sample were studied for frequency ranging from 0.1 to 500 $\text{rad}\cdot\text{s}^{-1}$ at 34°C, 37°C and 39°C, and the storage modulus (G') and loss modulus (G'') were shown below. A frequency dependent behavior was observed of SP1, in which for frequency values less than 1 $\text{rad}\cdot\text{s}^{-1}$, G' and G'' increased dramatically. Over the studied frequency range, G' was shown to be higher than G'' , suggesting the elasticity properties of SP1 at the three temperatures, as shown in Fig. S2a-c. While G'' was higher than G' of SP2 in whole frequency values from 0.1 to 300 $\text{rad}\cdot\text{s}^{-1}$, representing a typical viscous property of SP2 at the three temperatures (Fig. S2d-f). Similar to the SP1 sample, the 85:15 SP1:SP2 sample showed the elasticity properties from 1 to 500 $\text{rad}\cdot\text{s}^{-1}$ (Fig. S2g-i). These results exhibit that the 85:15 SP1:SP2 sample exists as an elastic material at 34-39 °C and is suitable for further preparation of composite materials with MWCNTs. The DMA characterization of the 85:15 sample also confirmed the result (Fig. S3).

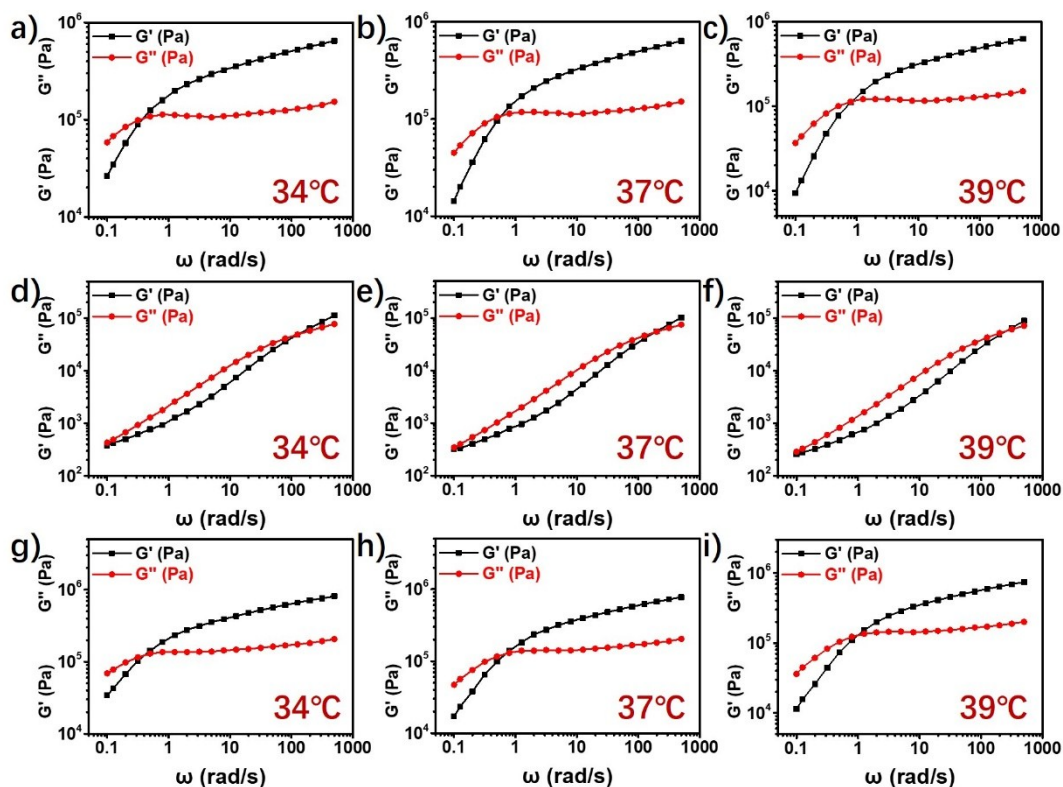


Fig. S2 Rheology studies of (a-c) SP1, (d-f) SP2 and (g-i) the 85:15 SP1:SP2 sample at different temperatures.

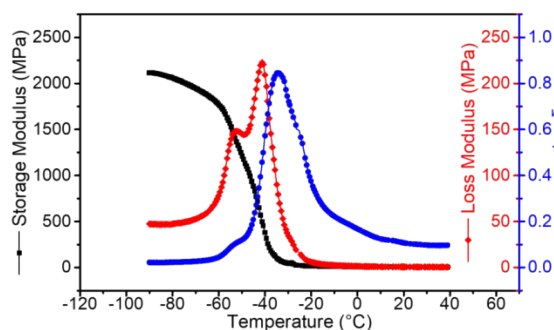


Fig. S3 DMA characterization of the 85:15 sample.

In order to confirm the stability of our MWCNT/supramolecular polymer composite film, rheology tests of 85:15 sample, conductivity-temperature test and stretching cycle testing of MWCNT/supramolecular polymer composite film had been carried out. As shown in Fig. S4a, the G' decreased and G'' increased as the temperature increasing, but G' was shown higher than G'' at 26°C–45°C, indicating the elasticity properties of the sample in this range of temperature. Viscoelasticity had changed within a range, which would promote the “wound” contacting to make self-healing possible without affecting sensor activity. Fig. S4b curves represented a stable

viscoelasticity for 2 hours at 34°C under 0.1% strain. During heating by thermal stages, the current remained at the same level when the temperature was below 42°C (Fig. S5). The relative resistance changes for stretching 75 cycles tests revealed excellent conductivity and mechanical property at room temperature (Fig. S6). According to the above results, we can make sure that our MWCNTs/supramolecular polymer composite films are stable enough in the working environments for sensing.

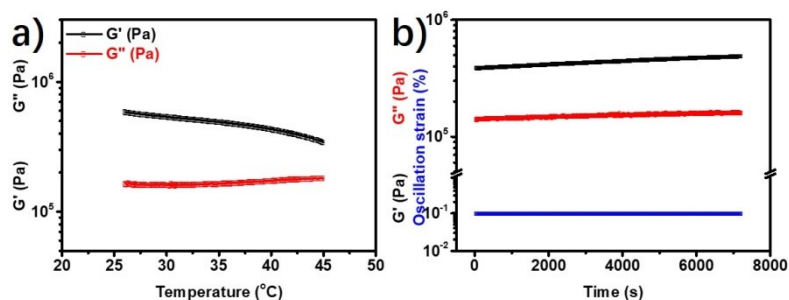


Fig. S4 Rheology tests of the 85:15 sample (a) 26°C~45°C, 0.1% strain, 1 Hz; (b) 34°C 0.1% strain, 1Hz.

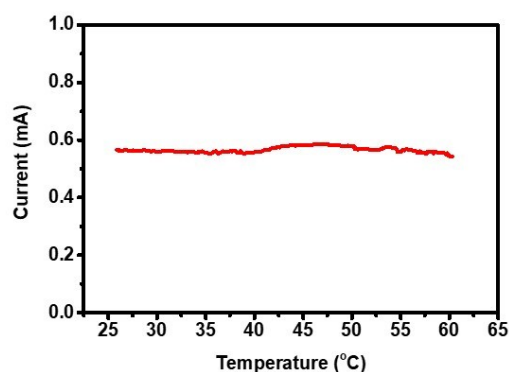


Fig. S5 Conductivity test of the MWCNT/supramolecular polymer composite film from 26°C~60°C (heating rate was set as 10°C/min).

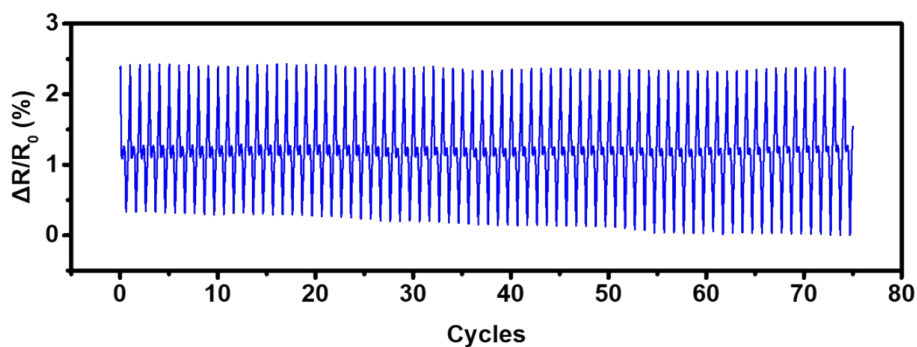


Fig. S6 The relative resistance changes for stretching cycle testing of MWCNT/supramolecular polymer composite film (2% ~10% strain, 1 Hz, room temperature, voltage 1.0 V).

3. Healing and sensing studies on the SP/MWCNTs composite films.

Before palm or NIR self-healing testing, the thermal responsive materials were self-repaired by Linkam thermal stages with 37°C (heating rate: 10 °C/min).

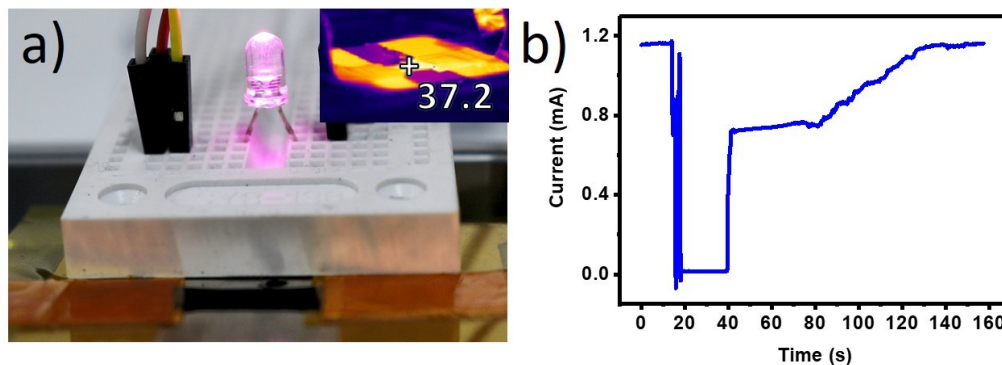


Fig. S7 The thermal stage self-healing test of the SP/MWCNTs composite films. a) The photo of thermal stage self-healing experiment. The thermal image of the sensor is inserted. The temperature of the center was about 37.2°C. b) The I-t curve of the thermal stage self-healing of the composite film. The film was recovered to the original property in about 130 seconds.

The conductive performance of the composite film after cutting and healing for 5 cycles was studied, as shown in Fig. S8. Whether it is cut or scratched, the conductivity can be well repaired after self-healing triggered by NIR irradiation. It should be noted that the conductivity couldn't recover completely (about 93.6% in current) after the fifth scratched. It is because the composite film was softened and became viscous after continuous NIR heating. The polymer with carbon nanotubes at the slit are stuck to the blade and taken away when cutting. The reduction of carbon nanotubes resulted in a slight decrease in current, but didn't affect the performance of the composite film.

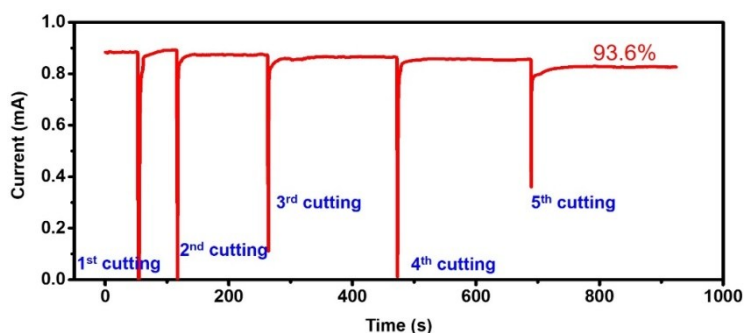


Fig. S8 The NIR triggered healing cycling investigation to the MWCNTs/supramolecular polymer composite film.

The 85:15 SP film is a hydrophobic surface with a contact angle of 94° , as shown in Fig. S9a. After spraying MWCNTs on the surface, the contact angle increased to 168° , indicating a superhydrophobic surface was obtained. As shown in Fig. S9, the MWCNTs were not all buried in the matrix and part of them existed on the surface of the composite film to form a more hydrophobic surface. At the same time, the spraying of the MWCNTs chloroform dispersion greatly increased the roughness of the surface of the composite film, thus contributing to the superhydrophobicity of composite film surface. This superhydrophobic surface endows the composite film with waterproof ability that facilitates the thermo-induced healing in underwater condition.

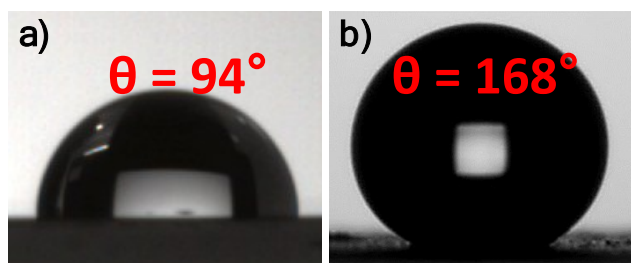


Fig. S9 The contact angle of (a) 85:15 SP1:SP2 sample and (b) the supramolecular polymer/MWCNTs composite film.

Owing to the sensor was an asymmetric film (only one side was coated with MWCNT), the sensing ability of different side up was evaluated (Fig. S10). When the MWCNT side attached to skin, the signal showed a slightly fluctuations that had little effect on using.

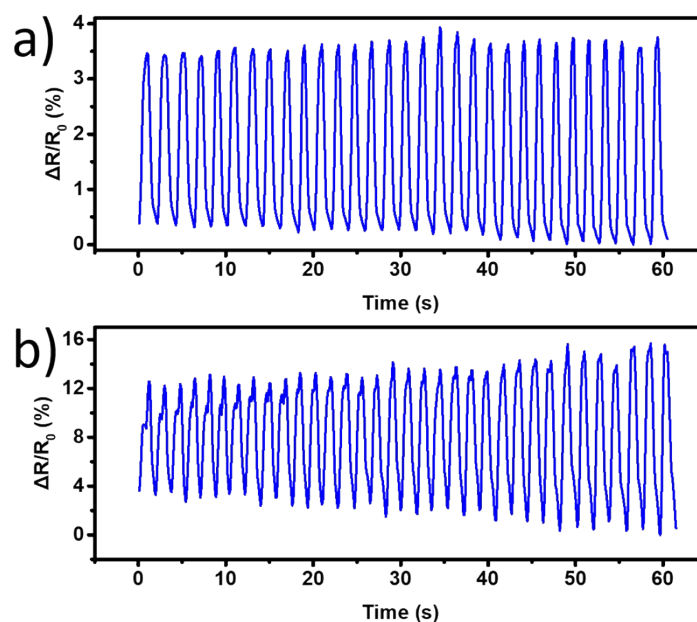


Fig. S10 The relative resistance change for finger bending. (a) MWCNT side up, (b) SP side up.

To further expanding healing methods, xenon lamp as simulated sunlight was also used for providing thermal energy. The results showed that a Xenon lamp can also make the film heal due based on the photo-thermal effect of MWCNTs components.

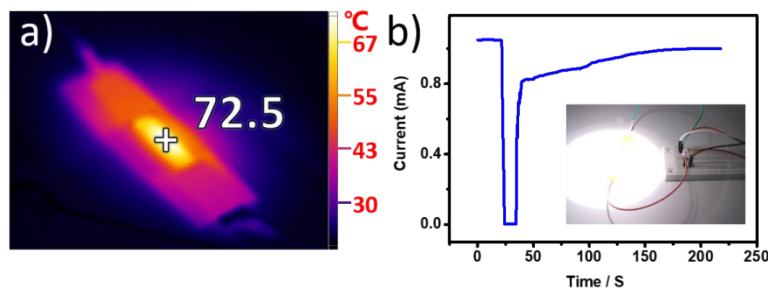


Fig. S11 The xenon lamp induced healing experiments of the composite films. (a) Thermal image of the sensor. The temperature of the center was about 72.5°C in 240 s. (b) The $I-t$ curve of the thermal stage self-healing of the sensor. The photo of healing experiment is shown in insert of (b).

Figure list:

Scheme S1 Synthetic route of supramolecular polymers.

Fig. S1 The FT-IR spectra of (a) SP1, (b) SP2, (c) 85:15 sample.

Fig. S2 The Rheology tests of (a-c) SP1, (d-f) SP2 and (g-i) the 85:15 sample at different temperatures.

Fig. S3 The DMA characterization of the 85:15 sample.

Fig. S4 The Rheology tests of the 85:15 sample.

Fig. S5 Conductivity test of the MWCNT/supramolecular polymer composite film from 26°C~60°C.

Fig. S6 The relative resistance changes for stretching cycle testing of MWCNT/supramolecular polymer composite film.

Fig. S7 The thermal stage self-healing test of the composite films.

Fig. S8 The NIR triggered healing cycling investigation to the MWCNTs/supramolecular polymer composite film.

Fig. S9 The contact angle of (a) 85:15 SP1:SP2 sample and (b) the supramolecular polymer/MWCNTs composite film.

Fig. S10 The relative resistance change for finger bending. (a) MWCNT side up (b) SP side up.

Fig. S11 The healing experiments of the composite films induced by a xenon lamp.